Heliyon 11 (2025) e41564

Contents lists available at ScienceDirect

Heliyon

journal homepage: www.cell.com/heliyon

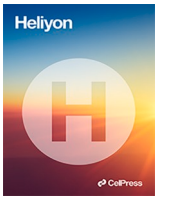

Research article

Glypican-3 is a key tuner of the Hedgehog pathway in COPD

Laure M.G. Petit [a], Lynda Saber Cherif [a], Maëva A. Devilliers [a], Sarah Hatoum [a], Julien Ancel [b], Gonzague Delepine [a], Anne Durlach [a], Xavier Dubernard [c], Jean-Claude Mérol [a], Christophe Ruaux [d], Myriam Polette [b], Gaëtan Deslée [b], Jeanne-Marie Perotin [b], Valérian Dormoy [a,*]

[a] Université de Reims Champagne-Ardenne, INSERM, P3Cell UMR-S1250, Reims, France
[b] Université de Reims Champagne-Ardenne, INSERM, CHU de Reims, P3Cell UMR-S1250, Reims, France
[c] Université de Reims Champagne-Ardenne, CHU de Reims, Reims, France
[d] Clinique Mutualiste La Sagesse, Département d'Otorhinolaryngologie, Rennes, France

ARTICLE INFO

Keywords:
COPD
Airway epithelial cells
Hedgehog
GPC3

ABSTRACT

Hedgehog (HH) pathway is involved in pulmonary development and lung homeostasis. It orchestrates airway epithelial cell (AEC) differentiation and contributes to respiratory pathogenesis. The core elements Gli2, Smo, and Shh were found altered in the bronchial epithelium of patients with chronic obstructive pulmonary disease (COPD). Here, we investigated the co-receptors to fully decipher the complex machinery of airway HH pathway activation in health and COPD. The core elements and co-receptors of HH signalling were investigated in lung cell populations using single-cell RNAseq analysis. The transcript levels of the principal co-receptor GPC3 were investigated on public RNAseq datasets and by RT-qPCR. The localisation of GPC3 was evaluated through immunofluorescent stainings on isolated bronchial AEC and tissues from non-COPD and COPD patients. GPC3 pharmacological modulation was achieved with Codrituzumab during AEC differentiation. We demonstrated that the core elements were not abundant in pulmonary cell populations. Focusing on co-receptors, GPC3 was the most expressed transcript in tracheobronchial epithelial cells. The decrease in GPC3 transcript levels correlated with the severity of airway obstruction in COPD patients. Finally, interfering with GPC3 signalling during AEC differentiation induced downregulation of the HH pathway attested by a decrease of Gli2 leading to reduced ciliogenesis and altered mucin production. GPC3 appears as a crucial co-receptor for the HH pathway in the respiratory context. The modulation of GPC3 may represent a novel experimental strategy to tune HH signalling in therapeutic perspectives.

1. Introduction

Chronic obstructive pulmonary disease (COPD) is currently the third leading cause of death in the world. Despite recent advances in patient phenotyping and understanding of the molecular and cellular components, clinical management is focused on symptoms and there are no available curative treatments. The epithelial remodelling of the airways is one of the main hallmarks of the

* Corresponding author. Inserm UMR-S 1250 University of Reims Champagne-Ardenne CHU Maison, Blanche 45 rue Cognacq-Jay 51092, Reims, France.
E-mail address: valerian.dormoy@univ-reims.fr (V. Dormoy).

https://doi.org/10.1016/j.heliyon.2024.e41564
Received 13 September 2024; Received in revised form 12 December 2024; Accepted 27 December 2024
Available online 28 December 2024
2405-8440/© 2024 The Authors. Published by Elsevier Ltd. This is an open access article under the CC BY-NC license (http://creativecommons.org/licenses/by-nc/4.0/).

physiopathology [1], particularly characterised by basal cell hyperplasia, ciliary defects, and an imbalance of mucin secretion [2–5]. It is observed and partially characterised at the bronchial, bronchiolar, and alveolar levels in association with COPD clinical features [6–9]. The origins of these alterations are not fully understood. To identify novel biomarkers and innovative therapies, it is necessary to decipher the mechanisms involved in the development of epithelial remodelling.

Hedgehog (HH) pathway is crucial for lung development, tissue repair, and regeneration [10–13]. The canonical HH pathway is initiated by the interaction of the ligand (Shh, Dhh, Ihh) with its receptor Ptch1 (Patched-1) resulting in Smoothened (Smo) activation. Finally, the transcription factors (Gli) are translocated into the nucleus, which triggers the transcription of target genes [14]. HH signalling defined by these core elements was found dysregulated in respiratory diseases [12,15,16]. Gli2, Smo, and Shh were reduced in airway epithelial cells from COPD patients. In addition, interfering with Shh signalling caused epithelial remodelling, such as ciliogenesis defects, impaired mucin abundance, and high proliferation of basal cells [17,18]. To date, mainly the core elements have been studied in the context of COPD. The molecular mechanisms regulating ligand release and signal reception have not been fully deciphered mainly because they involve a large panel of secondary elements (including BOC, CDON, DISP1, DISP2, GAS1, GAS8, GPC1, GPC3, GPC5, GPC6, GPR161, HHAT, HHIP, KIF7, PTCH2, SCUBE2, and SUFU) [14]. Interestingly, several single nucleotide polymorphisms (SNPs) of Hedgehog Interacting Protein (HHIP) were associated with COPD susceptibility and emphysema suggesting the importance of the secondary elements to relay a correct HH signalisation [19,20].

Here, we aimed to characterise the potential involvement of the HH pathway co-receptors in the development of COPD features in tissues and isolated airway epithelial cells. We focused on Cell adhesion molecule-related/down-regulated by oncogenes (CDON), Brother of CDON (BOC), Growth arrest-specific protein 1 (GAS1), Glypicans (GPC1, GPC3, GPC6), HHIP, and PTCH2.

2. Materials and methods

2.1. Single-cell sequencing dataset

The published single-cell sequencing (scRNAseq) can be found on the Cellxgene interface with “Sikkema et al.” dataset [21]. Only lung samples (lung and lung parenchyma) from subjects over 18 years without respiratory disease (n = 181) were considered. Four categories were defined regrouping cell populations as established by the HLCA (Human Lung Cell Atlas) consortium. The categories were identified as: (1) tracheobronchial epithelial cells (40,822 cells): ciliated columnar cell of tracheobronchial tree (25,114 cells),

Table 1
Clinical characteristics of patients.

Bronchial brushing			
	Non-COPD	COPD	
Number of subjects	11	11	
Gender F/M	4/7	2/9	ns
Age, years	55.5 ± 14.6	67.6 ± 7.2	*
Smoking history			
Never	0	0	
Former	5	6	ns
Current	6	5	ns
Pack-years	37 ± 26.5	58.1 ± 32.3	ns
Smoking cessation, years	7 ± 8	12.8 ± 17.6	ns
Lung functional parameters			
FEV_1 % pred	88.5 ± 10.6	58.5 ± 21.3	***
FEV_1/FVC	82.4 ± 6.9	57.1 ± 11.3	***
COPD			
GOLD 0/1/2/3/4		3/5/3/0	
FFPE tissues			
	Non-COPD	**COPD**	
Number of subjects	7	16	
Gender F/M	1/6	6/10	ns
Age, years	68.9 ± 6.8	62.3 ± 10.5	ns
Smoking history			
Never	0	0	
Former	5	9	ns
Current	2	7	ns
Pack-years	41 ± 27.8	46.6 ± 12.9	ns
Smoking cessation, years	13.3 ± 12.4	6.4 ± 8.4	ns
Lung functional parameters			
FEV_1 % pred	103.2 ± 12.4	76.3 ± 12	***
FEV_1/FVC	77.8 ± 3.4	61 ± 5.6	***
COPD			
GOLD 0/1/2/3/4		8/8/0/0	

Data are expressed as mean ± SD, number or percentage. FEV_1: Forced Expiratory Volume in 1s; FVC: Forced Capacity Capacity. Ns: non-significant; *$p < 0.05$; ***$p < 0.001$.

club cell (1816 cells) and respiratory basal cell (13,892 cells); (2) pneumocytes (123,456 cells): type I pneumocyte (19,418 cells) and type II pneumocyte (104,038 cells); (3) stromal cells (120,988 cells): alveolar type 1 fibroblast cell (21,389 cells), alveolar type 2 fibroblast cell (16,752 cells), bronchus fibroblast of lung (921 cells), capillary endothelial cell (37,538 cells), endothelial cell of lymphatic vessel (8675 cells), lung pericyte (5157 cells), myofibroblast cell (1048 cells), pulmonary artery endothelial cell (10,173 cells), tracheobronchial smooth muscle cell (5222 cells) and vein endothelial cell (14,113 cells); (4) immune cells (408,371 cells): B cell (6723 cells), CD1c-positive myeloid dendritic cell (10,628 cells), CD4-positive alpha-beta T cell (35,984 cells), CD8-positive alpha-beta T cell (43,839 cells), alveolar macrophage (174,329 cells), classical monocyte (33,862 cells), elicited macrophage (39, 642 cells), lung macrophage (6331 cells), mast cell (11,712 cells), natural killer cell (30,755 cells) and non-classical monocyte (14, 566). The median expression levels and the proportion of expressing cells for Hedgehog pathway markers are shown in a bubble plot generated by Rstudio with the ggplot2 package. The UMAP was generated with the CellxGene interface.

2.2. RNAseq analyses

Gene expressions of Hedgehog pathway elements were collected from datasets publicly available online (GEO database: GSE57148 and GSE137557). The gene expression profiling was obtained in lung tissues in the dataset GSE57148, and in submerged proliferative basal cells or fully differentiated cells in air-liquid interface cultures in the dataset GSE137557. COPD and non-COPD patients were included as described in the original publications with the clinical features listed in **Supplemental Materials:** Table S1 [22–26]. The analysis was performed on all genes and the differences between the two groups were determined using the Student's t-test and Benjamini-Hochberg FDR correction.

2.3. Human subjects

Patients scheduled for lung resection for cancer (University Hospital of Reims, France) (n = 23, Table 1) or for fiberoptic bronchoscopy with bronchial brushings (n = 22, Table 1) were prospectively recruited following standards established and approved by the institutional review board of the University Hospital of Reims, France (IRB Reims-CHU 20110612), and included in the cohort for research and innovation in chronic inflammatory respiratory disease (RINNOPARI, NCT02924818). The study included patients with or without COPD who gave their consent. Patients with other respiratory diseases (asthma, cystic fibrosis, bronchiectasis or pulmonary fibrosis) were excluded. At inclusion, age, sex, smoking history, and pulmonary function test results were recorded. COPD was defined by post-bronchodilator FEV_1 (forced expiratory volume in 1s)/FVC (forced vital capacity) < 0.7. Former smokers were considered for a smoking cessation longer than 6 months.

2.4. Human primary airway epithelial cell cultures

Isolated airway epithelial cells (AEC) were obtained from bronchial brushings (right lower lobe, 3rd to 5th order) of non-COPD (n = 7) and COPD patients (n = 7) to establish air-liquid interface (ALI) cultures as previously described for RNA extraction and cytospin processing [27]. The cells were recovered by scraping the brushes and dissociation using trypsin-versene (MS019B200D, Biowest). They were counted with ADAM (NanoEnTek) according to NanoEnTek instructions. 150,000 cells were seeded on 12-well plates containing 0.4 μm Transwells (Corning, Fisher Scientific) coated with 0.2 mg/mL collagen type IV from the human placenta (Sigma-Aldrich).

Human primary AEC were also obtained from nasal polyps resected from non-COPD patients (n = 5) at the University Hospital of Reims and the Clinic *La Sagesse* of Rennes to establish air-liquid interface (ALI) cultures as previously described for GPC3 modulation and whole-mount immunostaining [28]. Cells were dissociated by overnight pronase incubation (0.5 mg/mL, Sigma-Aldrich) and counted with ADAM (NanoEnTek) according to NanoEnTek instructions. One million cells were seeded on a 10 cm Petri dish until cell confluency. After a passage, 50,000 cells were seeded on 12-well plates containing 0.4 μm Transwells (Corning, Fisher Scientific) coated with 0.2 mg/mL collagen type IV from the human placenta (Sigma-Aldrich). Inhibition of GPC3 was achieved with Codrituzumab (HY-P99013, Interchim, diluted in sterile PBS, 1 μg/mL as described *in vitro* test) addition to the culture medium as indicated in the following figures [29].

CnT-17 media (CellnTec) was used for initial proliferation in apical and basal chambers. Upon reaching cell confluency, the apical medium was removed and PneumaCult-ALI (PnC-ALI, StemCell) medium was used in the basal chamber. The culture medium was changed every 2 days and cells were kept for 35 days in incubators at 37 °C, 5 % CO_2.

2.5. Cytospin

Fresh AEC were obtained from bronchial brushings of COPD (n = 7) and non-COPD patients (n = 7). Cells were recovered by scraping the brushes and dissociation using trypsin-versene (MS019B200D, Biowest). They were counted with ADAM (NanoEnTek) according to NanoEnTek instructions. 25,000 cells were centrifuged (800 rpm, 10min) with Cytospin4 (Microm Microtech) on a Superfrost® plus slide (Thermo Scientific) and fixed with ice-cold methanol for 10 min. Slides were stored at −20 °C until immunofluorescence analysis.

2.6. RT-qPCR analyses

Total RNA from AEC (ALI cultures from bronchial brushings) was isolated by GenElute RNA Plus purification Kit (RDP300, Sigma-Aldrich) and 250 ng were reverse-transcribed into cDNA by Maxima H Minus cDNA Synthetis Master Kit (MAN0016392, Thermo Scientific). Quantitative PCR reactions were performed with Luminaris Probe qPCR Master Kit (K0954, ThermoFisher) and Taqman Gene Expression Assay in a QuantStudio3 instrument (QS3, Thermo Scientific) as recommended by the manufacturer. The primers for GPC3 were purchased from ThermoFischer Scientific (Hs01018936_m1). The results for GPC3 transcript expressions were normalized to the expression of the housekeeping gene GAPDH (Hs02758991_g1) and expressed as ΔCT.

2.7. Cytospin immunofluorescent immunostaining

The cells were washed with PBS, blocked with 3 % BSA in PBS for 45 min, and then incubated with the primary antibody (listed in **Supplemental materials:** Table S2) for one night at 4 °C in 3 % BSA in PBS. After washing with PBS, a second primary antibody was used for 1h at room temperature. The cells were washed with PBS and incubated with the appropriate secondary antibodies in 3 % BSA in PBS for 30 min at room temperature. DNA was stained with DAPI during incubation for 15min. The micrographs were acquired by AxioImageur Zeiss (20x Ph) with ZEN software (8.1, 2012) and processed with ImageJ (National Institutes of Health) for analysis. Three random fields per slide were taken. For each field, a threshold was established by subtracting the background and setting the minimum at 0. GPC3 expression was determined by the whole cell pixel mean grey values (PMGV) of the detected antibody for 24 randomly selected multiciliated cells in the two groups.

2.8. Immunofluorescent staining and analyses

Immunofluorescent stainings were performed on formalin-fixed paraffin-embedded (FFPE) lung tissues distant from the tumour. Three μm sections were processed for these immunostainings. FFPE lung tissue section slides were deparaffinised and blocked with 10 % BSA in PBS for 30 min at room temperature. The tissue sections were then incubated with the primary antibody (listed in **Supplemental materials:** Table S2) for one night at 4 °C in 3 % BSA in PBS. After washing with PBS, a second primary antibody was used for 1h at room temperature. The sections were washed with PBS and incubated with the appropriate secondary antibodies in 3 % BSA in PBS for 30 min at room temperature. The DNA was stained with DAPI during incubation with the secondary antibodies. Micrographs were acquired by AxioImageur Zeiss (20x Ph) with ZEN software (8.1, 2012) and processed with ImageJ (National Institutes of Health) for analysis. For each patient, three random fields per section containing bronchi were taken to evaluate the localisation of GPC3 on epithelial cells. For each field, a threshold was established by subtracting the background, and setting the minimum at 0. GPC3 expression was determined by the pixel mean grey values (PMGV) in the selected region of interest defined by the entire epithelium in the two groups.

2.9. Whole-mount immunofluorescent immunostaining

Methanol-fixed AEC from ALI cultures were rehydrated by decreasing methanol concentration (75 %, 50 % and 25 %) before a post-fixation with acetone. The cells were blocked with 10 % BSA in PBT (PBS + 1 % DMSO + 0.1 % Triton) for 2 h at room temperature. The cells were then incubated with the primary antibody (listed in **Supplemental materials:** Table S2) for one night at 4 °C in 3 % BSA-PBT. After washing with PBT, the cells were incubated with the appropriate secondary antibodies in PBT for 2 h at room temperature. DNA was stained with DAPI during incubation for 15min. Clarification of cells was achieved by a glycerol gradient (25 %, 50 %, 75 %) before mounting the slides. Micrographs were acquired by AxioImageur Zeiss (40x Ph) with ZEN software (8.1, 2012) and processed with ImageJ (National Institutes of Health) for analysis. The pixel mean grey values (PMGV) for each detected antibody were quantified and compared between two groups for each staining.

2.10. Network of protein-protein interaction by string

The protein-protein interaction network for SHH (human) was generated by String (https://string-db.org/). Only the interactions with high confidence (0.7), experimentally determined or from curated databases are shown. No more than 10 interactors in the 1st shell and the 2nd shell are represented. The proteins were classified with a colour code: red for Shh, purple for Shh co-receptors and blue for GPC3.

2.11. Statistics

Data are expressed as mean values ± Standard deviation (SD) and percentages. Normality was assessed for each group using the Shapiro-Wilk test. Differences between the two groups were determined using the Student's t-test (two-tailed) for parametric data, Mann-Whitney for non-parametric data or the one-sample *t*-test compared with the hypothetical value of 1. The correlations were established with the Pearson test. A p-value <0.05 was considered significant; *, $p < 0.05$; **, $p < 0.01$.

3. Results

3.1. ScRNAseq highlights GPC3 as an essential co-receptor for the Hedgehog pathway in the airways

Considering the essential role of HH signalling in the respiratory system, we initially assessed the transcriptomic profile of HH core elements (DHH, IHH, SHH, GLI1, GLI2, GLI3, PTCH1, and SMO) and secondary co-receptors (BOC, CDON, GAS1, GPC1, GPC3, GPC5, GPC6, HHIP, PTCH2) at a cellular level. The selection of a large panel of immune cell populations indicated a low proportion of cells expressing HH pathway elements (0.6 ± 0.8 % [0.01–3.56]) (Fig. 1A). In the diverse category of stromal cells, HH pathway elements were present in 4 ± 4.5 % [0.03–17.69] of cells. Focusing on epithelial cells, the HH pathway elements were detected in 6.4 ± 11.5 % [0.03–47.03] of pneumocytes and 4.5 ± 5.4 % [0.05–20.21] of tracheobronchial epithelial cells. GPC5 and HHIP transcripts were the most abundant in pneumocytes (17.94 % and 47.03 % respectively). GPC5 was also the gene with the highest median of expression in this population (1.90). GPC3 was the most expressed gene in stromal cells (17.69 %) and tracheobronchial epithelial cells (20.21 %). Since the HH pathway is essential for airway epithelial cell differentiation, and GPC3 is the co-receptor showing the highest abundance in tracheobronchial epithelial cells, we next analysed its expression in the subsets of airway cell populations (Fig. 1B). Interestingly, GPC3 was mainly found in three populations: it was highly expressed in fibroblasts (51 %), multiciliated cells (26.83 %), and basal cells (10.79 %). This bioinformatics analysis prompted us to evaluate GPC3 as a key regulator of HH pathway signalling in COPD.

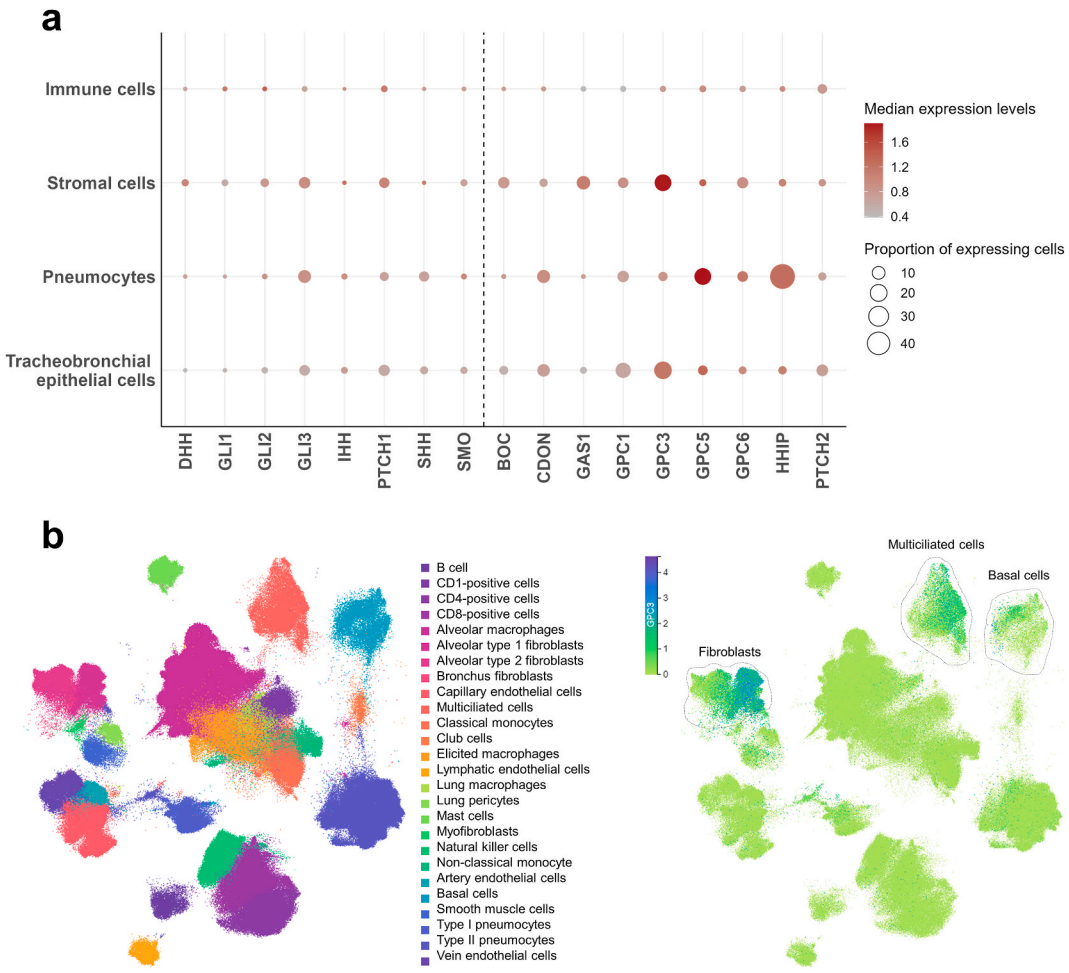

Fig. 1. Expression of GPC3 at a single-cell resolution in the human airways. (A) Bubble plot representing cell populations in y-axis and genes (regrouped in two categories: HH pathway core elements (DHH, GLI1, GLI2, GLI3, IHH, PTCH1, SHH, and SMO) and co-receptors (BOC, CDON, GAS1, GPC1, GPC3, GPC5, GPC6, HHIP, and PTCH2)) in x-axis. The size of the dots represents the proportion of expressing cells and the colour intensity represents the median of expression levels. Four categories of respiratory cell populations were selected: immune cells (n = 408371 cells), stromal cells (n = 120988 cells), pneumocytes (n = 123456 cells) and tracheobronchial epithelial cells (n = 40822 cells). (B) Left panel, UMAP of the HLCA pulmonary cell clusters. Right panel, UMAP of the GPC3 transcript levels for each cell population. The colour intensity represents the median of GPC3 transcript levels. The dashed lines highlight the population of fibroblasts, multiciliated cells, and basal cells.

3.2. GPC3 transcript levels are associated with pulmonary function in COPD patients

To determine the impact of GPC3 in COPD pathology, we analysed GPC3 transcript expressions in non-COPD and COPD patients. First, we investigated publicly available RNAseq data of current and former smoker mild, and moderate COPD patients (GSE57148) and very severe COPD patients (GSE137557). There was a decrease of 14.5 % in the expression of GPC3 in the whole lung of COPD patients (67.99 ± 34.21 FPKM vs 79.54 ± 35.05 FPKM, COPD vs non-COPD, $p < 0.05$) (Fig. 2A). Because bulk RNA sequencing data from whole lungs mainly represent non-epithelial cells, we explored a second dataset comprising cultured airway epithelial cells obtained from bronchial brushings of very severe COPD patients. GPC3 transcript expressions did not differ in proliferative basal cells (2.47 ± 0.75 FPKM vs 2.46 ± 0.36 FPKM, COPD vs non-COPD, $p > 0.05$) before the experimental switch in the air-liquid interface (Fig. 2B). However, there was a 61.6 % decrease of GPC3 transcripts at the end of cell differentiation (0.49 ± 0.22 FPKM vs 1.26 ± 0.27 FPKM, COPD vs non-COPD, $p < 0.01$).

Since GPC3 is not solely expressed by airway epithelial cells (Figs. 1A and 2A), and very severe COPD patients are highly heterogeneous (Fig. 2B), we secondly analysed GPC3 transcripts in cultured airway epithelial cells collected during bronchial brushing in mild to severe COPD patients (Fig. 3). During the early steps of epithelial cell differentiation (ALI7), there was no difference in GPC3 transcript expressions between non-COPD and COPD samples (9.29 ± 1.32ΔCt vs 9.10 ± 1.08ΔCt, COPD vs non-COPD, $p > 0.05$) (Fig. 3A). There was no correlation between GPC3 transcript levels and FEV_1 in COPD patients ($r^2 = 0.4349$, $p > 0.05$) (Fig. 3B). Interestingly, low GPC3 transcript expressions in COPD patients were correlated with low pulmonary functional parameters defined by FEV_1/FVC ($r^2 = 0.8419$, $p < 0.01$) (Fig. 3C). In fully differentiated epithelia (ALI35), GPC3 transcript expressions did not differ between COPD and non-COPD patients (8.26 ± 1.48ΔCt vs 8.33±1ΔCt, COPD vs non-COPD, $p > 0.05$) (Fig. 3D). Importantly, there was an association between GPC3 transcript levels and lung function in COPD: the patients with low FEV_1 and FEV_1/FVC harboured low GPC3 transcript levels ($r^2 = 0.7013$, $p < 0.05$ and $r^2 = 0.9486$, $p < 0.001$, respectively) (Fig. 3E and F). In addition, there was no association with the pack-years. Altogether, these findings suggest a decrease in GPC3 transcript levels in association with the severity of lung function impairment in COPD patients. The transcript levels of GPC3 may act as a sensor contributing to epithelial remodelling during COPD development.

3.3. The localisation of GPC3 is altered in COPD patients

We first investigated GPC3 protein levels and localisations in airway multiciliated cells from bronchial brushings of non-COPD and COPD patients. GPC3 was mainly localised in the sub-ciliary compartment (Fig. 4A). We did not observe a significant modification of GPC3 localisation between COPD and non-COPD patients (901.8 ± 253.2 PMGV vs 1110 ± 400.4 PMGV, COPD vs non-COPD, $p > 0.05$) (Fig. 4B). There was no association between FEV_1 or FEV_1/FVC of COPD patients and GPC3 abundance in multiciliated cells ($r^2 = 0.1864$, $p > 0.05$ and $r^2 = 0.1608$, $p > 0.05$, respectively) (Fig. S1). In addition, there was no association with the pack-years.

We then analysed GPC3 protein levels and localisations in the bronchial epithelia of FFPE lung tissues. We confirmed the presence of GPC3 preferentially in differentiated cells, localised in cilia and cytoplasm (Fig. 5A). There was a 30.3 % decrease in GPC3 localisation in COPD patients (2664 ± 872.4PMGV vs 3820 ± 983.5PMGV, COPD vs non-COPD, $p < 0.05$) (Fig. 5B). Nonetheless, there

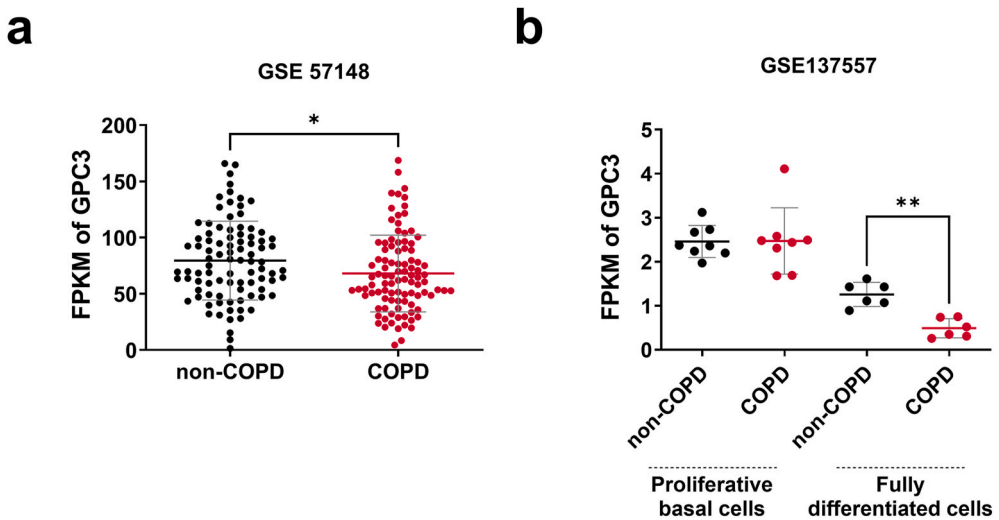

Fig. 2. GPC3 transcript levels are decreased in COPD patients. (A) Dot plot with mean ± SD showing GPC3 expression analysis from RNAseq data (GSE57148). The whole-lung tissues were obtained from COPD (n = 98, red) and non-COPD (n = 91, black) patients. *$p < 0.05$; non-COPD vs COPD. (B) Dot plot with mean ± SD showing GPC3 expression analysis from RNAseq data (GSE137557). The airway epithelial cells were obtained from tracheobronchial segments of non-COPD and COPD patients and cultured in air-liquid interface conditions. The proliferative basal cells (n = 8) were collected for analysis in submerged conditions before the air switch and the fully differentiated cells (n = 6) were collected for analysis after 28 days of differentiation. **$p < 0.01$; non-COPD vs COPD. FPKM: Fragments per kilobase million.

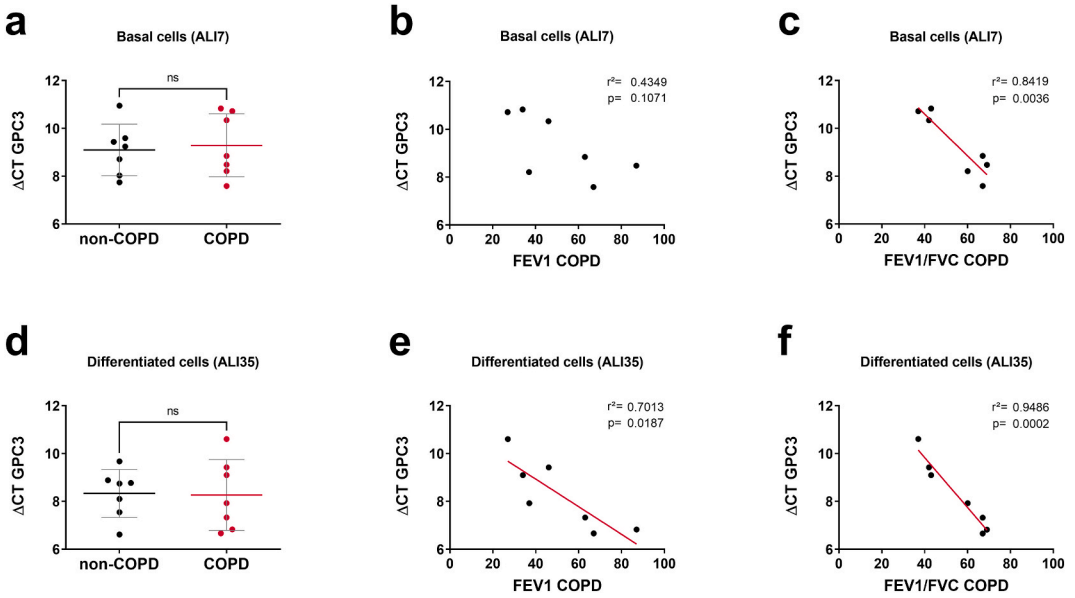

Fig. 3. GPC3 transcript levels are associated with lung function in COPD patients. ALI cultures were performed from isolated AEC obtained from COPD patients (n = 7, red) and non-COPD (n = 7, black), and collected for transcript analysis after 7 days (basal cells) or 35 days (differentiated cells). (A) Dot plot with mean ± SD showing ΔCT GPC3 expression analysis on basal cells. ns: non-significant; non-COPD vs COPD. (B) Linear regression representing a correlation between GPC3 transcript levels and FEV_1 (forced expiratory volume in 1s) in ALI7 cultures of COPD patients (n = 7). (C) Linear regression representing a correlation between GPC3 transcript levels and FEV_1/FVC (forced vital capacity) in ALI7 cultures of COPD patients. (D) Dot plot with mean ± SD showing GPC3 expression analysis on differentiated cells. ns: non-significant; non-COPD vs COPD. (E) Linear regression representing a correlation between GPC3 transcript levels and FEV_1 in ALI35 cultures of COPD patients (n = 7). (F) Linear regression representing a correlation between GPC3 transcript levels and FEV_1/FVC in ALI35 cultures of COPD patients.

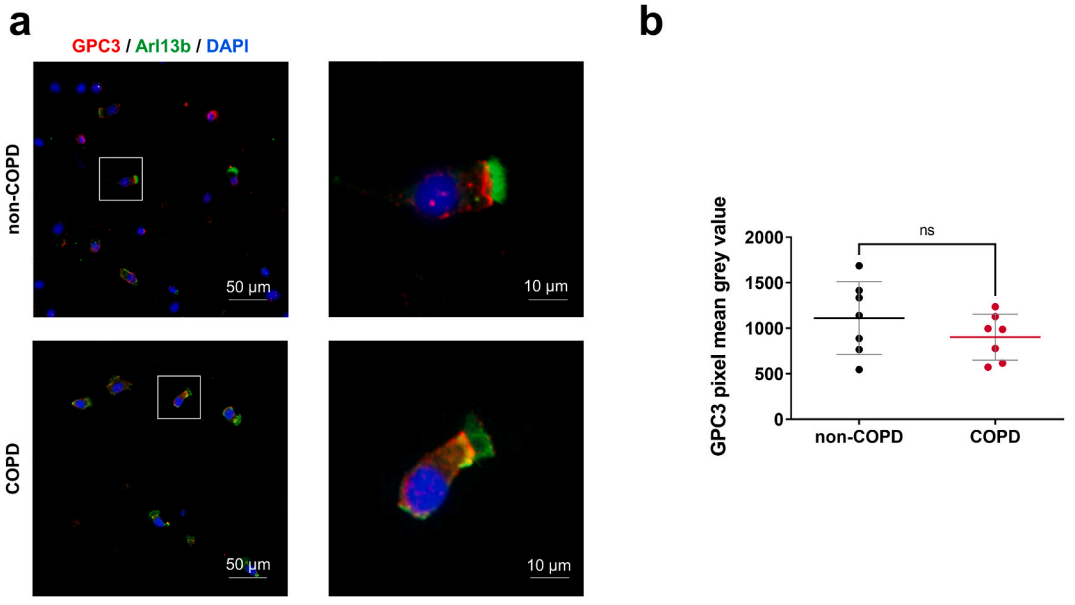

Fig. 4. Localisation of GPC3 in isolated AEC of non-COPD and COPD patients. (A) Representative micrographs taken from cytospun AEC of non-COPD and COPD patients showing cilia (Arl13b, green) and GPC3 (red). Nuclei are stained in blue (DAPI). Magnification corresponding to the selected area is shown. (B) Dot plot with mean ± SD representing GPC3 pixel mean grey values of non-COPD (n = 7, black) and COPD (n = 7, red) patients. ns: non-significant; non-COPD vs COPD.

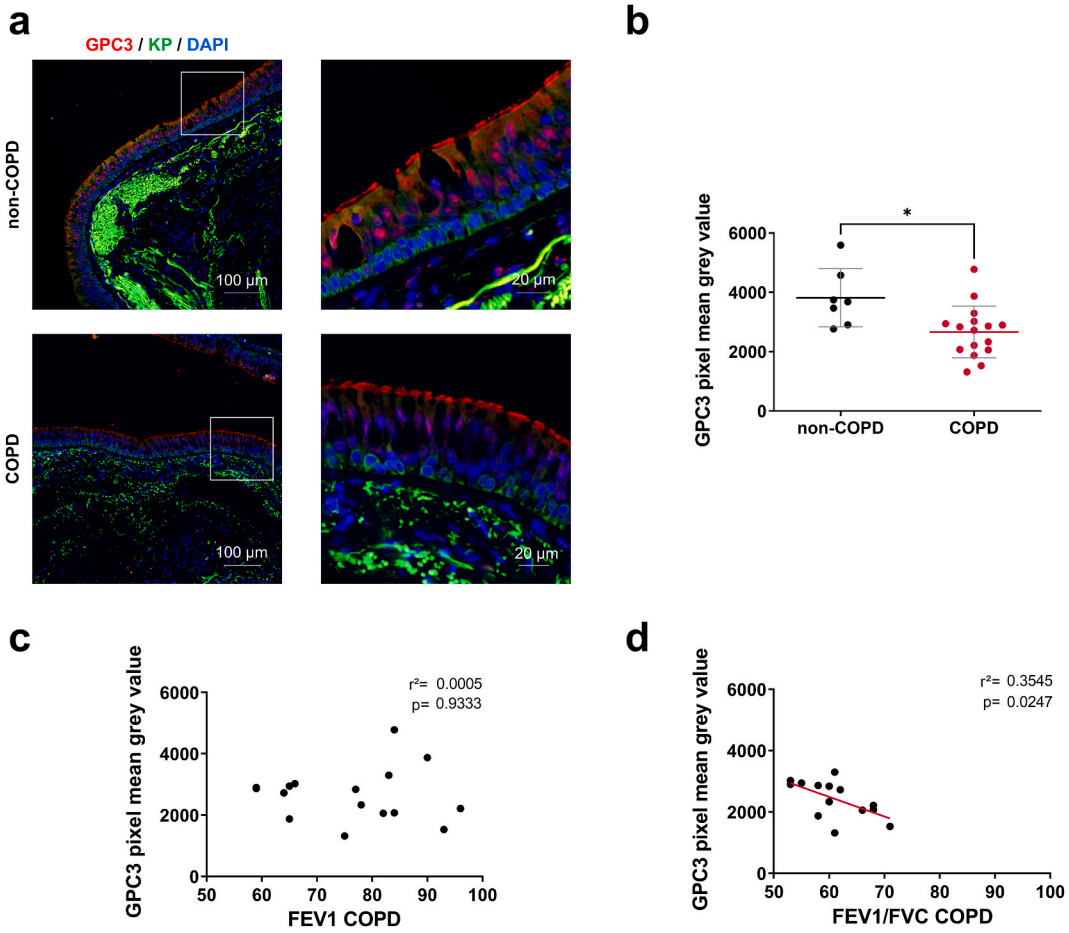

Fig. 5. Localisation of GPC3 on FFPE lung tissues of non-COPD and COPD patients. (A) Representative micrographs showing bronchial epithelia of non-COPD and COPD patients stained for GPC3 (red), basal cells (KP, green) and cell nuclei (DAPI, blue). Magnification corresponding to the selected area is shown. (B) Dot plot with mean ± SD representing GPC3 pixel mean grey values of non-COPD (n = 7, black) and COPD (n = 16, red) patients. *$p < 0.05$; non-COPD vs COPD. (C) Linear regression representing a correlation between GPC3 pixel levels and FEV_1 in bronchial epithelia of COPD patients (n = 16). (D) Linear regression representing a correlation between GPC3 pixel levels and FEV_1/FVC in bronchial epithelia of COPD patients (n = 14).

was no correlation between FEV_1 or FEV_1/FVC in COPD patients and GPC3 epithelial abundance (Fig. 5C and D). In addition, there was no association with the pack-years. Taken together, GPC3 protein levels are decreased in the epithelial cells of COPD patients.

3.4. *Interfering with GPC3 signalling induced epithelial remodelling*

Considering the HH pathway is involved in airway epithelial remodelling and the co-receptor GPC3 is altered in COPD patients, we evaluated the impact of GPC3 modulation *in vitro* resorting to the well-described surrogate of AEC from nasal polyps [17,30–33]. We selected a monoclonal antibody directed against GPC3 (Codrituzumab, also known as GC33) to interfere with GPC3 transduction signals [29,34]. We verified the effects of the pharmacological modulation on the GPC3 protein: Codrituzumab did not influence the GPC3 protein levels between the two conditions at the end of the differentiation (Fold Change 1.13 ± 0.24, Codrituzumab vs control, $p > 0.05$) (Fig. S2).

Firstly, we built a protein-protein interaction network for SHH and GPC3 (Fig. 6A) showing the links between the HH ligands, the receptors, the co-receptors, and the potential other interactors. Because we identified an association with the Wnt pathway, we examined β-catenin staining as a readout. There was no difference in β-catenin localisation between cells treated with Codrituzumab and untreated (Fig. S3). The proportion of basal cells (p63 positive cells) or their proliferative status (Ki67 positive cells) during differentiation (ALI7) was also not affected by GPC3 modulation (Fold Change 1.16 ± 0.38 and 1.12 ± 0.45, Codrituzumab vs control, $p > 0.05$, respectively) (Figs. S4 and S5).

We next assessed the molecular effects of GPC3 inhibition on the HH pathway signalling. Gli2 protein levels were reduced in Codrituzumab-treated cells at an early stage of differentiation (Fold Change 0.59 ± 0.25, Codrituzumab vs control, $p < 0.05$) but not at a late stage (Fold Change 0.89 ± 0.25, Codrituzumab vs control, $p > 0.05$) (Fig. 6B and C).

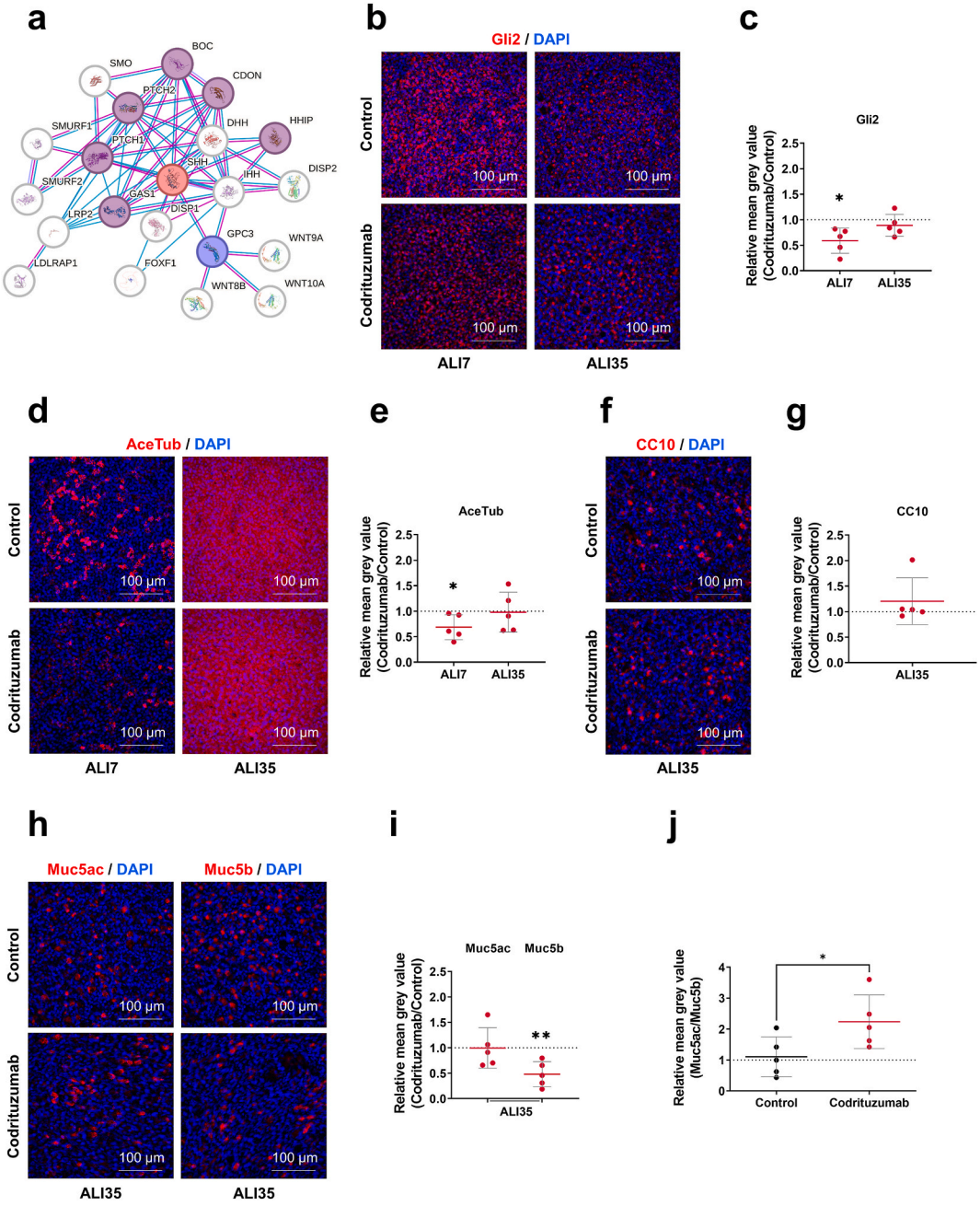

Fig. 6. GPC3 inhibition by Codrituzumab alters AEC differentiation. (A) Network of protein-protein interaction generated on the Search Tool for the Retrieval of Interacting Genes/Proteins (STRING). (B) Representative micrographs taken from AEC cultures codrituzumab-treated or untreated at ALI7 and ALI35 stained for Gli2 (red) and cell nuclei (blue). (C) Dot plot with mean ± SD showing relative pixel mean grey values of Gli2 at ALI7 and ALI35. *$p < 0.05$; Control vs Codrituzumab. (D) Representative micrographs of AEC cultures codrituzumab-treated or untreated at ALI7 and ALI35 showing cilia (Acetylated tubulin, red) and cell nuclei (blue). (E) Dot plot with mean ± SD showing relative pixel mean grey values of acetylated tubulin at ALI7 and ALI35. *$p < 0.05$; Control vs Codrituzumab. (F) Representative micrographs of AEC cultures codrituzumab-treated or untreated at ALI35 stained for CC10 (red) and cell nuclei (blue). (G) Dot plot with mean ± SD showing relative pixel mean grey values of CC10 at ALI35 in Codrituzumab-treated conditions compared to untreated cultures. (H) Representative micrographs taken from AEC cultures codrituzumab-treated or untreated at ALI35 stained for mucins (Muc5ac or Muc5b, red) and cell nuclei (blue). (I) Dot plot with mean ± SD showing relative pixel mean grey values of Muc5ac or Muc5b at ALI35. **$p < 0.01$; Control vs Codrituzumab. (J) Dot plots with mean ± SD representing the relative pixel mean grey value ratios of Muc5ac/Muc5b in untreated (black) and Codrituzumab-treated cells (red). *$p < 0.05$; Control vs Codrituzumab.

Finally, we investigated the epithelial remodelling induced by GPC3 modulation. A regular microscopic inspection of the cultures until ALI35 did not show evidence of changes in global architecture, epithelial thickness, or cell density. Interestingly, Codrituzumab treatment induced a reduction of multiciliated cells at ALI7 (Fold Change 0.69 ± 0.24, Codrituzumab vs control, $p < 0.05$) that did not persist at ALI35 (Fold Change 0.98 ± 0.39, Codrituzumab vs control, $p > 0.05$) (Fig. 6D and E). Focusing on the secreting cell populations, we did not observe a modification of CC10 protein levels (Fold Change 1.20 ± 0.46, Codrituzumab vs control, $p > 0.05$) (Fig. 6F and G). However, Muc5b protein levels were significantly reduced in Codrituzumab-treated cells (Fold Change 0.48 ± 0.25, Codrituzumab vs control, $p < 0.01$), while Muc5ac protein levels did not differ (Fold Change 0.99 ± 0.40, Codrituzumab vs control, $p > 0.05$) (Fig. 6H and I). In addition, the ratios Muc5ac/Muc5b were increased when GPC3 signalling was altered (2.24 ± 0.86 vs 1.11 ± 0.65, Codrituzumab vs control, $p < 0.05$) (Fig. 6J). In summary, interfering with GPC3 signalling during AEC differentiation impaired HH pathway activation and induced epithelial remodelling.

4. Discussion

We identified GPC3 as a crucial regulator of HH signalling in the respiratory context with transcriptional and localisation alterations in COPD patients. We also highlighted the involvement of GPC3 in epithelial remodelling and HH signalling in the lung.

The exploration of the scRNAseq from the HLCA has been recently very successful in identifying transcripts of interest and establishing a molecular print of cells in the respiratory system [21]. This dataset includes the major scRNAseq analyses of respiratory samples already published to represent the large diversity of lung cell populations. Interestingly, the transcript levels of the core elements of the HH pathway were not abundant, whereas the co-receptors reached up to 47.03 % of expressing cells in pneumocytes. This is consistent with the recent and only partial elucidation of the plethora of HH pathway molecular effectors: if the core elements are necessary for the activation, the secondary elements including, in particular, the co-receptors are essential for the fine-tuning of the signal transduction [14,35–37]. GPC3 appeared as a novel candidate in the complex machinery involving the HH pathway to control respiratory homeostasis. Therefore, we dissected its molecular signature in the context of COPD where we previously demonstrated the involvement of the HH pathway in the associated epithelial remodelling [17].

There was a decrease of GPC3 transcripts in the whole lung of mild and moderate COPD patients, as well as in fully differentiated AEC from severe COPD patients in ALI culture. Interestingly, GPC3 transcript levels correlated exclusively with the respiratory function in COPD patients suggesting that COPD patient heterogeneity also emerged through the lens of HH pathway co-receptors. Consequently, GPC3 protein levels were found significantly reduced in the epithelium of the bronchi of COPD patients. Even if the localisation appeared mainly on multiciliated cells in the tissues, there was no statistically significant reduction of GPC3 on isolated multiciliated cells from COPD patients. A complex subcellular microscopic analysis may help decipher the molecular signal transduction and its alteration in COPD since intracellular regional localisation and concentration gradients are often described for HH components [10,12,38].

Our experimental design showed for the first time that the blockage of GPC3 signalling using Codrituzumab altered the HH pathway activation in the respiratory context without impacting the Wnt pathway during the initiation of AEC differentiation. In addition, we demonstrated that preventing GPC3 signalling induced an alteration of ciliogenesis and mucin production mimicking the epithelial remodelling described in COPD bronchi [4,5]. These findings will require confirmation in AEC isolated and cultured from non-COPD and COPD bronchial brushings. For instance, Muc5b is a major element of the epithelial defence in the lung as illustrated by the $Muc5b^{-/-}$ mice lacking a proper mucociliary clearance and therefore more sensitive to infections [39]. These findings complete our previous investigations focusing on the HH core elements where the alteration of the HH pathway was highlighted in COPD patients [17,18]. The decrease in Gli2 and Shh that we originally described may be partly due to a dysfunction of GPC3 signalling in these patients preventing the binding of the ligand to the co-receptor for optimal activation and therefore downregulating the HH pathway.

GPC3 is a heparan sulfate proteoglycan bound to the cell membrane by glycosyl-phosphatidyl-inositol (GPI) anchor that can undergo cleavage by Furin-like protein forming a pocket for binding various substrates [40]. Consequently, GPC3 is an ideal co-receptor that occupies a restricted space at the cell membrane, binds specifically to Shh, and can release the ligand for the extracellular compartment or to a nearby receptor. GPC3 regulates cell proliferation, apoptosis, and epithelial-mesenchymal transition in various cancers, such as hepatocellular carcinoma, breast cancer or lung cancer [41–43]. The involvement of GPC3 in HH signalling seems to be context-dependent and has not been explored in the respiratory system so far. Investigations on developmental models such as the $GPC3^{-/-}$ mouse reported that Shh can bind to GPC3 inducing ligand endocytosis and inhibition of the HH pathway by competition with Ptch1 [44,45]. Our results are in accordance with a recent study that demonstrated the necessity of Shh bound on heparin sulfate chains of GPC3 for HH pathway activation as illustrated by a decrease of Gli1 and Gli2 in primary cilia of mouse embryonic $GPC3^{-/-}$ fibroblasts [46].

Despite the novelty and the multi-level cellular and molecular characterisation of GPC3 that we report, our study presents some limitations. We focused on the bronchial epithelium of COPD patients either current smokers or former smokers. Nonetheless, COPD is also a small airway disease characterised by an important inflammation [3,47]. Expanding the experimental approaches on the bronchiolar and alveolar compartments, as well as mimicking the inflammation and the cigarette smoke exposure will provide important clues to improve the understanding of the HH pathway activation in respiratory research. We selected GPC3 but the synergy with other glypicans such as GPC5 abundant in pneumocytes, or other co-receptors like CDON may also unveil additional modulators of the HH pathway. GPC3 was found highly expressed in fibroblasts but we did not explore this aspect while the literature indicated an upregulation of GPC3 in cancer-associated fibroblasts, and an activation of fibroblasts by the HH pathway in the context of idiopathic lung fibrosis [48,49]. Interestingly, with the advent of RNA therapeutics and cellular targeting, it could be possible to restore GPC3

signalling to prevent COPD-associated epithelial remodelling as microRNAs controlling GPC3 expression such as miR129-1-3P, miR1303, and miR1291 have already been identified [50,51].

In conclusion, we reported the first analysis of the transcript levels of HH co-receptors in the lung. *Ex vivo* and *in vitro* analysis highlighted the involvement of GPC3 in airway epithelial remodelling and its alteration in COPD patients. Understanding the mechanisms of GPC3 regulation in HH signalling is crucial to consider GPC3 as a potential biomarker or therapeutic strategy in the context of COPD.

CRediT authorship contribution statement

Laure M.G. Petit: Writing – review & editing, Writing – original draft, Visualization, Validation, Methodology, Investigation, Formal analysis. **Lynda Saber Cherif:** Writing – review & editing, Investigation, Formal analysis, Conceptualization. **Maëva A. Devilliers:** Writing – review & editing, Investigation, Formal analysis. **Sarah Hatoum:** Writing – review & editing, Investigation, Formal analysis. **Julien Ancel:** Writing – review & editing, Resources, Investigation, Formal analysis, Data curation. **Gonzague Delepine:** Writing – review & editing, Resources, Investigation, Data curation. **Anne Durlach:** Writing – review & editing, Resources, Data curation. **Xavier Dubernard:** Writing – review & editing, Resources, Investigation. **Jean-Claude Mérol:** Writing – review & editing, Resources, Investigation. **Christophe Ruaux:** Writing – review & editing, Resources, Investigation. **Myriam Polette:** Writing – review & editing, Funding acquisition. **Gaëtan Deslée:** Writing – review & editing, Resources, Methodology, Investigation, Formal analysis, Data curation. **Jeanne-Marie Perotin:** Writing – review & editing, Writing – original draft, Visualization, Validation, Supervision, Resources, Project administration, Methodology, Investigation, Funding acquisition, Formal analysis, Data curation, Conceptualization. **Valérian Dormoy:** Writing – review & editing, Writing – original draft, Visualization, Validation, Supervision, Project administration, Methodology, Investigation, Funding acquisition, Formal analysis, Data curation, Conceptualization.

Ethics approval and consent to participate

Non-COPD and COPD patients were recruited from the Department of Pulmonary Medicine at the University Hospital of Reims (France) and included in the Research and Innovation in Chronic Inflammatory Respiratory Diseases (RINNOPARI, NCT02924818) cohort. The study was approved by the ethics committee (CCP Dijon EST I, N°2016-A00242–49) and was conducted in accordance with the ethical guidelines of the Declaration of Helsinki. The study included patients who gave their written informed consent to participate.

Data sharing

RNAseq and scRNAseq data were obtained through publicly available depositories and interfaces. All data generated or analysed during this study are included in this published article. Additional data are available upon request to the corresponding author.

Funding

The University of Reims Champagne-Ardenne (URCA) and the French National Institute of Health and Medical Research (Inserm) funded this research.

Declaration of competing interest

The authors declare the following financial interests/personal relationships which may be considered as potential competing interests:Julien Ancel reports a relationship with Amgen France that includes: consulting or advisory and funding grants. Julien Ancel reports a relationship with Roche that includes: consulting or advisory and travel reimbursement. Julien Ancel reports a relationship with Pfizer France that includes: consulting or advisory and travel reimbursement. Julien Ancel reports a relationship with MSD that includes: consulting or advisory and travel reimbursement. Julien Ancel reports a relationship with Bristol-Myers Squibb France that includes: consulting or advisory. Julien Ancel reports a relationship with Novartis that includes: consulting or advisory. Julien Ancel reports a relationship with astrazeneca that includes: consulting or advisory. Julien Ancel reports a relationship with takeda that includes: consulting or advisory. Julien Ancel reports a relationship with sanofi that includes: consulting or advisory and travel reimbursement. Julien Ancel reports a relationship with Regeneron Pharmaceuticals Inc that includes: consulting or advisory and travel reimbursement. Gaetan Deslee reports a relationship with Nuvaira Inc that includes: consulting or advisory. Gaetan Deslee reports a relationship with PneumRx that includes: consulting or advisory. Gaetan Deslee reports a relationship with chiesi that includes: consulting or advisory. Gaetan Deslee reports a relationship with Boehringer Ingelheim Ltd that includes: consulting or advisory. Gaetan Deslee reports a relationship with AstraZeneca that includes: consulting or advisory. Jeanne-Marie Perotin reports a relationship with AstraZeneca that includes: speaking and lecture fees and travel reimbursement. Jeanne-Marie Perotin reports a relationship with chiesi that includes: travel reimbursement. Valerian Dormoy reports a relationship with AstraZeneca that includes: consulting or advisory, funding grants, and travel reimbursement. If there are other authors, they declare that they have no known competing financial interests or personal relationships that could have appeared to influence the work reported in this paper.

Acknowledgments

We thank the members of the Inserm UMR-S 1250 unit and our collaborators for their helpful comments and insights. We thank the Platform of Cell and Tissue Imaging (PICT) for technical assistance. We thank Clinic *La Sagesse* for their collaboration in sample collection.

Appendix A. Supplementary data

Supplementary data to this article can be found online at https://doi.org/10.1016/j.heliyon.2024.e41564.

References

[1] A. Agustí, B.R. Celli, G.J. Criner, D. Halpin, A. Anzueto, P. Barnes, et al., Global initiative for chronic obstructive lung disease 2023 report: GOLD executive summary, Eur. Respir. J. 61 (2023) 2300239, https://doi.org/10.1183/13993003.00239-2023.
[2] R.G. Crystal, Airway basal cells. The "smoking gun" of chronic obstructive pulmonary disease, Am. J. Respir. Crit. Care Med. 190 (2014) 1355–1362, https://doi.org/10.1164/rccm.201408-1492PP.
[3] M. Saetta, G. Turato, S. Baraldo, A. Zanin, F. Braccioni, C.E. Mapp, et al., Goblet cell hyperplasia and epithelial inflammation in peripheral airways of smokers with both symptoms of chronic bronchitis and chronic airflow limitation, Am. J. Respir. Crit. Care Med. 161 (2000) 1016–1021, https://doi.org/10.1164/ajrccm.161.3.9907080.
[4] G. Radicioni, A. Ceppe, A.A. Ford, N.E. Alexis, R.G. Barr, E.R. Bleecker, et al., Airway mucin MUC5AC and MUC5B concentrations and the initiation and progression of chronic obstructive pulmonary disease: an analysis of the SPIROMICS cohort, Lancet Respir. Med. 9 (2021) 1241–1254, https://doi.org/10.1016/S2213-2600(21)00079-5.
[5] S. Gohy, F.M. Carlier, C. Fregimilicka, B. Detry, M. Lecocq, M.Z. Ladjemi, et al., Altered generation of ciliated cells in chronic obstructive pulmonary disease, Sci. Rep. 9 (2019) 17963, https://doi.org/10.1038/s41598-019-54292-x.
[6] F. Xu, D.M. Vasilescu, D. Kinose, N. Tanabe, K.W. Ng, H.O. Coxson, et al., The molecular and cellular mechanisms associated with the destruction of terminal bronchioles in COPD, Eur. Respir. J. 59 (2022) 2101411, https://doi.org/10.1183/13993003.01411-2021.
[7] A. Higham, A.M. Quinn, J.E.D. Cançado, D. Singh, The pathology of small airways disease in COPD: historical aspects and future directions, Respir. Res. 20 (2019) 49, https://doi.org/10.1186/s12931-019-1017-y.
[8] A. Higham, S. Booth, J. Dungwa, D. Singh, Histopathology of the small airways: Similarities and differences between ageing and COPD, Pulmonology 31 (1) (2024), https://doi.org/10.1080/25310429.2024.2430032.
[9] A. Higham, J. Dungwa, N. Jackson, D. Singh, Relationships between airway remodeling and clinical characteristics in COPD patients, Biomedicines 10 (2022) 1992, https://doi.org/10.3390/biomedicines10081992.
[10] M. Zhang, H. Wang, H. Teng, J. Shi, Y. Zhang, Expression of SHH signaling pathway components in the developing human lung, Histochem. Cell Biol. 134 (2010) 327–335, https://doi.org/10.1007/s00418-010-0738-2.
[11] R. Belgacemi, S. Danopoulos, G. Deutsch, I. Glass, V. Dormoy, S. Bellusci, et al., Hedgehog signaling pathway orchestrates human lung branching morphogenesis, Int. J. Mol. Sci. 23 (2022) 5265, https://doi.org/10.3390/ijms23095265.
[12] C. Wang, NSR de Mochel, S.A. Christenson, M. Cassandras, R. Moon, A.N. Brumwell, et al., Expansion of hedgehog disrupts mesenchymal identity and induces emphysema phenotype, J. Clin. Invest. 128 (2018) 4343–4358, https://doi.org/10.1172/JCI99435.
[13] T. Peng, D.B. Frank, R.S. Kadzik, M.P. Morley, K.S. Rathi, T. Wang, et al., Hedgehog actively maintains adult lung quiescence and regulates repair and regeneration, Nature 526 (2015) 578–582, https://doi.org/10.1038/nature14984.
[14] K. Petrov, B.M. Wierbowski, A. Salic, Sending and receiving hedgehog signals, Annu. Rev. Cell Dev. Biol. 33 (2017) 145–168, https://doi.org/10.1146/annurev-cellbio-100616-060847.
[15] A.L. Bolaños, C.M. Milla, J.C. Lira, R. Ramírez, M. Checa, L. Barrera, et al., Role of Sonic Hedgehog in idiopathic pulmonary fibrosis, Am. J. Physiol. Lung Cell Mol. Physiol. 303 (2012) L978–L990, https://doi.org/10.1152/ajplung.00184.2012.
[16] A. Tam, E.T. Osei, C.Y. Cheung, M. Hughes, C.X. Yang, K.M. McNagny, et al., Hedgehog signaling as a therapeutic target for airway remodeling and inflammation in allergic asthma, Cells 11 (2022) 3016, https://doi.org/10.3390/cells11193016.
[17] R. Belgacemi, E. Luczka, J. Ancel, Z. Diabasana, J.-M. Perotin, A. Germain, et al., Airway epithelial cell differentiation relies on deficient Hedgehog signalling in COPD, EBioMedicine 51 (2020) 102572, https://doi.org/10.1016/j.ebiom.2019.11.033.
[18] J. Ancel, R. Belgacemi, J.-M. Perotin, Z. Diabasana, S. Dury, M. Dewolf, et al., Sonic hedgehog signalling as a potential endobronchial biomarker in COPD, Respir. Res. 21 (2020) 207, https://doi.org/10.1186/s12931-020-01478-x.
[19] S.G. Pillai, D. Ge, G. Zhu, X. Kong, K.V. Shianna, A.C. Need, et al., A genome-wide association study in chronic obstructive pulmonary disease (COPD): identification of two major susceptibility loci, PLoS Genet. 5 (2009) e1000421, https://doi.org/10.1371/journal.pgen.1000421.
[20] X. Zhou, R.M. Baron, M. Hardin, M.H. Cho, J. Zielinski, I. Hawrylkiewicz, et al., Identification of a chronic obstructive pulmonary disease genetic determinant that regulates HHIP, Hum. Mol. Genet. 21 (2012) 1325–1335, https://doi.org/10.1093/hmg/ddr569.
[21] L. Sikkema, C. Ramírez-Suástegui, D.C. Strobl, T.E. Gillett, L. Zappia, E. Madissoon, et al., An integrated cell atlas of the lung in health and disease, Nat. Med. 29 (2023) 1563–1577, https://doi.org/10.1038/s41591-023-02327-2.
[22] I. Jeong, J.-H. Lim, D.K. Oh, W.J. Kim, Y.-M. Oh, Gene expression profile of human lung in a relatively early stage of COPD with emphysema, Int. J. Chronic Obstr. Pulm. Dis. 13 (2018) 2643–2655, https://doi.org/10.2147/COPD.S166812.
[23] S. Vishweswaraiah, L. George, N. Purushothaman, K. Ganguly, A candidate gene identification strategy utilizing mouse to human big-data mining: "3R-tenet" in COPD genetic research, Respir. Res. 19 (2018) 92, https://doi.org/10.1186/s12931-018-0795-y.
[24] W.J. Kim, J.H. Lim, J.S. Lee, S.-D. Lee, J.H. Kim, Y.-M. Oh, Comprehensive analysis of transcriptome sequencing data in the lung tissues of COPD subjects, Int J Genomics 2015 (2015) 206937, https://doi.org/10.1155/2015/206937.
[25] E.S. McCluskey, N. Liu, A. Pandey, N. Marchetti, S.G. Kelsen, U.S. Sajjan, Quercetin improves epithelial regeneration from airway basal cells of COPD patients, Respir. Res. 25 (2024) 120, https://doi.org/10.1186/s12931-024-02742-0.
[26] F. Pineau, G. Shumyatsky, N. Owuor, N. Nalamala, S. Kotnala, S. Bolla, et al., Microarray analysis identifies defects in regenerative and immune response pathways in COPD airway basal cells, ERJ Open Res 6 (2020) 656–2020, https://doi.org/10.1183/23120541.00656-2020.
[27] L. Saber Cherif, Z. Diabasana, J.-M. Perotin, J. Ancel, L.M.G. Petit, M.A. Devilliers, et al., The nicotinic receptor polymorphism rs16969968 is associated with airway remodeling and inflammatory dysregulation in COPD patients, Cells 11 (2022) 2937, https://doi.org/10.3390/cells11192937.
[28] Z. Diabasana, J.-M. Perotin, R. Belgacemi, J. Ancel, P. Mulette, C. Launois, et al., Chr15q25 genetic variant rs16969968 alters cell differentiation in respiratory epithelia, Int. J. Mol. Sci. 22 (2021) 6657, https://doi.org/10.3390/ijms22136657.
[29] K. Nakano, T. Orita, J. Nezu, T. Yoshino, I. Ohizumi, M. Sugimoto, et al., Anti-glypican 3 antibodies cause ADCC against human hepatocellular carcinoma cells, Biochem. Biophys. Res. Commun. 378 (2009) 279–284, https://doi.org/10.1016/j.bbrc.2008.11.033.

[30] L. Müller, L.E. Brighton, J.L. Carson, W.A. Fischer, I. Jaspers, Culturing of human nasal epithelial cells at the air liquid interface, J. Vis. Exp. 50646 (2013), https://doi.org/10.3791/50646.
[31] A.A. Pezzulo, T.D. Starner, T.E. Scheetz, G.L. Traver, A.E. Tilley, B.-G. Harvey, et al., The air-liquid interface and use of primary cell cultures are important to recapitulate the transcriptional profile of in vivo airway epithelia, Am. J. Physiol. Lung Cell Mol. Physiol. 300 (2011) L25–L31, https://doi.org/10.1152/ajplung.00256.2010.
[32] S. Ruiz García, M. Deprez, K. Lebrigand, A. Cavard, A. Paquet, M.-J. Arguel, et al., Novel dynamics of human mucociliary differentiation revealed by single-cell RNA sequencing of nasal epithelial cultures, Dev Camb Engl 146 (2019) dev177428, https://doi.org/10.1242/dev.177428.
[33] J.J. Brewington, E.T. Filbrandt, F.J. LaRosa, J.D. Moncivaiz, A.J. Ostmann, L.M. Strecker, et al., Brushed nasal epithelial cells are a surrogate for bronchial epithelial CFTR studies, JCI Insight 3 (2018) e99385, https://doi.org/10.1172/jci.insight.99385, 99385.
[34] T. Ishiguro, M. Sugimoto, Y. Kinoshita, Y. Miyazaki, K. Nakano, H. Tsunoda, et al., Anti-glypican 3 antibody as a potential antitumor agent for human liver cancer, Cancer Res. 68 (2008) 9832–9838, https://doi.org/10.1158/0008-5472.CAN-08-1973.
[35] B.M. Wierbowski, K. Petrov, L. Aravena, G. Gu, Y. Xu, A. Salic, Hedgehog pathway activation requires coreceptor-catalyzed, lipid-dependent relay of the sonic hedgehog ligand, Dev. Cell 55 (2020) 450–467.e8, https://doi.org/10.1016/j.devcel.2020.09.017.
[36] J. Svärd, K. Heby-Henricson, M. Persson-Lek, B. Rozell, M. Lauth, A. Bergström, et al., Genetic elimination of Suppressor of fused reveals an essential repressor function in the mammalian Hedgehog signaling pathway, Dev. Cell 10 (2006) 187–197, https://doi.org/10.1016/j.devcel.2005.12.013.
[37] E. Petrova, J. Rios-Esteves, O. Ouerfelli, J.F. Glickman, M.D. Resh, Inhibitors of hedgehog acyltransferase block sonic hedgehog signaling, Nat. Chem. Biol. 9 (2013) 247–249, https://doi.org/10.1038/nchembio.1184.
[38] E. Simon, A. Aguirre-Tamaral, G. Aguilar, I. Guerrero, Perspectives on intra- and intercellular trafficking of hedgehog for tissue patterning, J. Dev. Biol. 4 (2016) 34, https://doi.org/10.3390/jdb4040034.
[39] M.G. Roy, A. Livraghi-Butrico, A.A. Fletcher, M.M. McElwee, S.E. Evans, R.M. Boerner, et al., Muc5b is required for airway defence, Nature 505 (2014) 412–416, https://doi.org/10.1038/nature12807.
[40] B. De Cat, S.-Y. Muyldermans, C. Coomans, G. Degeest, B. Vanderschueren, J. Creemers, et al., Processing by proprotein convertases is required for glypican-3 modulation of cell survival, Wnt signaling, and gastrulation movements, J. Cell Biol. 163 (2003) 625–635, https://doi.org/10.1083/jcb.200302152.
[41] M. Capurro, I.R. Wanless, M. Sherman, G. Deboer, W. Shi, E. Miyoshi, et al., Glypican-3: a novel serum and histochemical marker for hepatocellular carcinoma, Gastroenterology 125 (2003) 89–97, https://doi.org/10.1016/s0016-5085(03)00689-9.
[42] F.O. Alshammari, A.O. Satari, A.S. Aljabali, Y.S. Al-mahdy, Y.J. Alabdallat, Y.M. Al-sarayra, et al., Glypican-3 differentiates intraductal carcinoma and paget's disease from other types of breast cancer, Medicina (Mex) 59 (2023) 86, https://doi.org/10.3390/medicina59010086.
[43] J. Ning, S. Jiang, X. Li, Y. Wang, X. Deng, Z. Zhang, et al., GPC3 affects the prognosis of lung adenocarcinoma and lung squamous cell carcinoma, BMC Pulm. Med. 21 (2021) 199, https://doi.org/10.1186/s12890-021-01549-9.
[44] M.I. Capurro, W. Shi, J. Filmus, LRP1 mediates Hedgehog-induced endocytosis of the GPC3-Hedgehog complex, J. Cell Sci. 125 (2012) 3380–3389, https://doi.org/10.1242/jcs.098889.
[45] M.I. Capurro, P. Xu, W. Shi, F. Li, A. Jia, J. Filmus, Glypican-3 inhibits Hedgehog signaling during development by competing with patched for Hedgehog binding, Dev. Cell 14 (2008) 700–711, https://doi.org/10.1016/j.devcel.2008.03.006.
[46] Y.C. Liu, B.M. Wierbowski, A. Salic, Hedgehog pathway modulation by glypican 3-conjugated heparan sulfate, J. Cell Sci. 135 (2022) jcs259297, https://doi.org/10.1242/jcs.259297.
[47] J.C. Hogg, F. Chu, S. Utokaparch, R. Woods, W.M. Elliott, L. Buzatu, et al., The nature of small-airway obstruction in chronic obstructive pulmonary disease, N. Engl. J. Med. 350 (2004) 2645–2653, https://doi.org/10.1056/NEJMoa032158.
[48] D. Li, Y. Wang, C. Shi, S. Fu, Y.-F. Sun, C. Li, Targeting GPC3high cancer-associated fibroblasts sensitizing the PD-1 blockage therapy in gastric cancer, Ann. Med. 55 (2023) 2189295, https://doi.org/10.1080/07853890.2023.2189295.
[49] W.I. Effendi, T. Nagano, The hedgehog signaling pathway in idiopathic pulmonary fibrosis: resurrection time, Int. J. Mol. Sci. 23 (2022) 171, https://doi.org/10.3390/ijms23010171.
[50] M. Maurel, S. Jalvy, Y. Ladeiro, C. Combe, L. Vachet, F. Sagliocco, et al., A functional screening identifies five microRNAs controlling glypican-3: role of miR-1271 down-regulation in hepatocellular carcinoma, Hepatol Baltim Md 57 (2013) 195–204, https://doi.org/10.1002/hep.25994.
[51] M. Maurel, N. Dejeans, S. Taouji, E. Chevet, C.F. Grosset, MicroRNA-1291-mediated silencing of IRE1α enhances Glypican-3 expression, RNA N Y N 19 (2013) 778–788, https://doi.org/10.1261/rna.036483.112.